Preprints.org

Article

Nanofibrous ε-Polycaprolactone Matrices Containing Nano-Hydroxyapatite and Humulus lupulus L. Extract: Physicochemical and Biological Characterization for Drug Delivery Applications

Jaime A Villanueva-Lumbreras , Ciro Rodriguez [*] , María Rosa Aguilar , Hamlet Aviles-Arnaut ,
Geoffrey A. Cordell , Aida Rodriguez-Garcia [*]

Article

Nanofibrous ε-Polycaprolactone Matrices Containing Nano-Hydroxyapatite and *Humulus lupulus* L. Extract: Physicochemical and Biological Characterization for Drug Delivery Applications

Jaime Villanueva-Lumbreras [1], Ciro Rodriguez [2,3,*], María Rosa Aguilar [4,5], Hamlet Aviles-Arnaut [1], Geoffrey A. Cordell [6] and Aida Rodriguez-Garcia [1,2,*]

[1] Universidad Autónoma de Nuevo León, Facultad de Ciencias Biológicas, Instituto de Biotecnología, Ave. Pedro de Alba S/N, Ciudad Universitaria, San Nicolás de los Garza, NL, 66455, Mexico; J.V.-L, javillanueva6@hotmail.com; H.A.-A, hamlet.avilesarn@uanl.edu.mx

[2] Tecnologico de Monterrey, Escuela de Ingeniería y Ciencias, Ave. Eugenio Garza Sada 2501, Monterrey, NL, 64849, Mexico; ciro.rodriguez@tec.mx

[3] Laboratorio Nacional de Manufactura Aditiva y Digital (MADIT), Apodaca, NL, 66629, Mexico.

[4] Instituto de Ciencia y Tecnología de Polímeros (ICTP-CSIC), 28006 Madrid, Spain; mraguilar@ictp.csic.es

[5] Networking Biomedical Research Centre in Bioengineering, Biomaterials and Nanomedicine, CIBER.BBN, 28029 Madrid, Spain; mraguilar@ictp.csic.es

[6] Natural Products Inc., Evanston, IL, 60201, USA and College of Pharmacy, University of Florida, Gainesville, FL, 32610, USA; pharmacog@gmail.com

* Correspondence: A.R.-G.: aida.rodriguezgrc@uanl.edu.mx; C.R.: ciro.rodriguez@tec.mx.

Abstract: Oral bone defects occur as a result of trauma, cancer, infections, periodontal diseases, and caries. Autogenic and allogenic grafts are the gold standard used to treat and regenerate damaged or defective bone segments. However, these materials do not possess the antimicrobial properties necessary to inhibit the invasion of the numerous deleterious pathogens present in the oral microbiota. In the present study poly(ε-caprolactone) (PCL), nano-hydroxyapatite (nHAp), and a commercial extract of *Humulus lupulus* L. (hops) were electrospun into polymeric matrices to assess their potential for drug delivery and bone regeneration. The fabricated matrices were analyzed by scanning electron microscopy (SEM), tensile analysis, thermogravimetric analysis (TGA), FT-IR assay, and in vitro hydrolytic degradation. The antimicrobial properties were evaluated against the oral pathogens *Streptococcus mutans*, *Porphyromonas gingivalis*, and *Aggregatibacter actinomycetemcomitans*. The cytocompatibility was proved by the MTT assay. SEM analysis proved the nanostructured matrices have suitable fiber size. The present research provides new information about the interaction of natural compounds with ceramic and polymeric biomaterials. The hop extract and other natural or synthetic medicinal agents can be effectively loaded into PCL fibers and has the potential to be used in biomedical applications.

Keywords: poly(ε-caprolactone); electrospinning; nano-hydroxyapatite; *Humulus lupulus*; hops; drug delivery system; bone regeneration

1. Introduction

Advances in the field of biomaterials and nanotechnology have revolutionized traditional therapeutic modalities to improve the functionality of drug delivery and tissue engineering [1]. Biomaterials are a critical element in the development of scaffolds that provide a three-dimensional niche to mimic the extracellular matrix (ECM), and facilitate cell migration, proliferation, and vascularization, which are essential elements during tissue regeneration [2]. An adequate scaffold for bone regeneration should possess several properties relating to biocompatibility, biodegradability,

porosity, and osteoinductivity [3] to promote bone growth, and to provide temporary mechanical support in the bone defect area. Biocompatibility allows the cells to adhere to a scaffold without stimulating an undesirable immune response, and to proliferate into regenerated functional tissue. That is a principal objective of tissue engineering wherein, over time, the human cells replace the implanted scaffold through the production of new tissue. A porous scaffold with adequate mechanical properties permits cell migration and the formation of a structure that can support manipulation during the surgical process and subsequently until tissue regeneration is complete [4].

Poly(ε-caprolactone) (PCL) is a biocompatible and biodegradable polymer employed as a support matrix for the fabrication of scaffolds which encompass active adjuvants [5]. It is widely used in tissue regeneration applications due to its ease of handling applying a variety of processing techniques [6], however it possesses poor mechanical and osteoconductivity properties. To overcome these limitations, the incorporation of inorganic components into the polymeric matrices, such as bioactive glasses and ceramics, e.g., hydroxyapatite, improve the mechanical strength and foster osteoconduction during the bone regeneration processes [7–9]. In addition, modification of the scaffolds through the incorporation of bioactive compounds improves their functionality [10], and acts as a highly targeted delivery system for medicinal agents which stimulates and guides the cellular regeneration process, while concomitantly inhibiting both microbial infection and transplant rejection [11].

Hydroxyapatite ($Ca_{10}(OH)_2(PO_4)_6$) provides important biological characteristics, including being a part of the bone matrix and promoting bone cell differentiation, which can assist during the mineralization process, and as an osteoconductive material can be used in the area requiring bone regeneration [12,13].

Bone loss in the oral cavity may occur as the result of trauma, cancer, congenital diseases, periodontal diseases, and caries [14]. Periodontitis is an infectious and inflammatory disease caused mainly by the Gram-negative bacteria *Porphyromonas gingivalis* and *Aggregatibacter actinomycetemcomitans*. It is an important disease that causes tooth loss in humans through the progressive destruction of the tissues supporting the teeth [15]. Caries, a multifactorial infectious disease results in the demineralization of dental hard tissues and the loss of teeth. The primary causative agent associated with dental caries is *Streptococcus mutans*, a microorganism that can form biofilms [16]. A common failure of the existing scaffolds for oral applications following surgery is subsequent microbial infection which inhibits tissue generation [17]. One possible solution is to fabricate scaffolds that, through the incorporation of antimicrobial agents, have the capacity to inhibit microbial infection [18].

Natural products incorporated into scaffolds have been investigated for their synergistic action in combination with biomaterials for bone regeneration and the prevention of infection [18]. Due to the increase in microbial multidrug resistance (MDR) to many front-line antibiotics, the search for antimicrobial metabolites from plants has gained interest [19]. *Humulus lupulus* L. (known as hops) is member of the Cannabaceae family and was originally from Western Asia. Now it is naturalized in central Europe and is widely cultivated in North and South America, South Africa, and Australia [20]. The bitter metabolites produced by the flower-heads (cones) are used in the brewing industry for their organoleptic properties that improve the flavor and aroma of beer [21]. Due to the rich composition of hop cones, they have long been used as a valuable raw material in a variety of applications. The secondary metabolites, the bitter acids, the polyphenols, and the essential oil components, have demonstrated anticancer and anti-inflammatory properties; antibacterial, antifungal, and anticancer activities; and anti-inflammatory, anticancer, and analgesic effects, respectively [20].

Extracts of hop cones have been evaluated for their antimicrobial properties against oral Streptococci, particularly *S. mutans*, *S. sanguis*, and *S. salivarius* [22,23]. The principal metabolites characterized from hops: humulone, isohumulone, lupulone, and xanthohumol, have demonstrated anti-inflammatory [24], antimicrobial [25], and anticancer activities, and inhibition of bone resorption [26]. Xanthohumol, an important prenylated chalconoid derivative in the female inflorescence of

hops, enhances osteoblast differentiation at concentrations of 0.001, 0.01, 0.1, and 1µg/mL [27]. The extract used in the present research was a commercial CO_2-prepared hop extract (Hopsteiner).

Of the fabrication techniques employed to develop scaffolds, electrospinning is a simple process which produces nanofibers considered to be a highly effective platform for biomedical applications for drug release, wound healing, and tissue engineering [28]. Electrospinning enables the combination of biomaterials to generate nanofiber membranes through the application of variable manufacturing parameters. In addition, it is a method for the fabrication of porous, three-dimensional, delivery systems of synthetic and natural compounds to introduce biological properties into the matrix for diverse applications [29,30].

This study was designed to fabricate and characterize membranes of PCL nanofibers loaded with nanohydroxyapatite and the hop extract, produced through electrospinning, and to evaluate their physicochemical, mechanical, and *in vitro* antimicrobial and cytotoxic properties, prior to consideration for the bone-targeted delivery of medicinal agents.

2. Materials and Methods

2.1. Materials

Poly(ε-caprolactone) pellets (Mw = 80,000 Da) and hydroxyapatite (nanopowder <200 nm particle size) were purchased from Sigma Aldrich (St. Louis, MO, USA). The *Humulus lupulus* L. extract containing mainly 83.2% of α-bitter acids (humulone) and 97.3% of β-bitter acids (lupulone), and 90% of xanthohumol was obtained from the Hopsteiner Company (New York, NY, USA). The hop extract was diluted in methanol to prepare the stock solution with a final concentration of 10 mg/mL. The extract was stored at 4°C in the dark until used. Acetone and methanol were purchased from CTR Scientific S.A de C.V (Monterrey, NL, Mexico), and syringes were purchased from Becton Dickinson (Franklin Lakes, NJ, USA).

2.2. Fabrication of Electrospun Nanofibers

The matrices were fabricated using an electrospinning apparatus composed of a high voltage source of power (Gamma High Voltage Research, Ormond Beach, FL, USA), a syringe infusion pump (KD Scientific, Holliston, MA, USA) fitted with a metallic blunt-tip 27G needle (CML Supply, Lexington, KY, USA), and a 5-mL plastic syringe (BD Plastipak™, Franklin Lakes, NJ, USA). The polymeric solutions were prepared with PCL 9% w/v, using acetone as the solvent and stirred overnight at room temperature. The different concentrations of nanohydroxyapatite were 1, 3, and 5% w/v, while the hop extract was added in concentrations of 1, 3, and 5% v/v. The solutions were stirred for 24 h at room temperature, individually transferred into the syringe, injected with the infusion pump, and electrospun under optimized parameters (0.4 mL/h flow rate, 15 cm distance from the needle tip to the collector, and 25 kV) at room temperature and at 50% relative humidity. The fibers were collected and deposited in a 10 x 10 cm metallic collector covered by non-stick aluminum foil. During the experiments, the relative humidity was 50% and the temperature was 25°C. The samples obtained from the electrospinning technique were dried under vacuum for 48 h to complete solvent removal. The conferred names for the samples are related to their composition. Thus, the PCL samples were composed of only PCL, the PCL+nHAp samples were composed of PCL and nanohydroxyapatite, and the PCL+nHAp+hop extract samples were composed of PCL, nanohydroxyapatite, and the hop extract.

2.3. Morphological Characterization

Examinations of the morphology and the overall fiber distribution of the electrospun matrices were carried out with a scanning electron microscope Philips XL30 SEM TMP (F.E.I. Company, Hillsboro, OR, USA). The samples were covered with a sputtered gold film (Polaron SC7640, Newhaven, UK) and observed in the SEM. The average fiber diameter and distribution were analyzed using ImageJ software (National Institutes of Health, Bethesda, MD, USA).

2.4. Thermogravimetric Analysis

Thermogravimetric analysis (TGA) of the electrospun matrices was carried out in a Thermogravimetric Analyzer TA Q500 (New Castle, DE, USA), from room temperature to 600°C, 10°C/min^{-1} under a nitrogen atmosphere.

2.5. Fourier-transform Infrared Spectroscopy (FTIR) Analysis

The functional groups present in the PCL, nHap, and hop extracts were analyzed by FTIR analysis using a Perkin Elmer FTIR spectrometer (Waltham, MA, USA) in the range 4000–400 cm^{-1}.

2.6. Mechanical Characterization

The mechanical properties of the obtained matrices were determined with a universal testing machine (Instron 3345, Worthing, Sussex, UK). Rectangular samples (3 × 10 mm) were cut and mounted between holders and tested (n = 8) under dry conditions. The results were reported as mean ± standard deviation (SD).

2.7. In vitro Degradation Assays

The degradation tests were performed in accordance with ISO 10993-13: 2010 [31]. Triplicate samples (~10 mg) of the electrospun matrices were immersed in sterile flasks with 100 mL of phosphate-buffered saline (PBS) at pH ~7.4 at 37°C, with constant agitation at 120 rpm for 8 weeks. After each immersion period was concluded, the samples were removed and washed three times with distilled water to remove salt residues, dried for under vacuum to constant mass and weighed.

The percentage weight loss was calculated using the following equation:

$$\text{Weight loss (\%)} = \frac{(Wi - Wf)}{Wi} \times 100$$

Where Wi is the initial sample weight and Wf is the final sample weight after degradation at different time periods.

2.8. Antibacterial Assay

The *in vitro* antibacterial activity of the acquired hop extract was evaluated against the oral pathogenic organisms *Streptococcus mutans* (Sm) (ATCC 700610), *Porphyromonas gingivalis* (Pg) (ATCC 33277), and *Aggregatibacter actinomycetemcomitans* (Aa) (ATCC 43718) through measuring the zones of inhibition using the agar diffusion assay [32]. *S. mutans* was cultured on brain heart infusion (BHI) (Becton Dickinson, Sparks, MD, USA) for 24 h at 37°C and 5% CO_2, while *P. gingivalis* and *A. actinomycetemcomitans* were cultured on tryptic soy broth (TSB) (Becton Dickinson, Monterrey, NL, Mexico) for 24 h at 37°C under anaerobic conditions. Microbial suspensions with an optical density of 0.5 McFarland standard at 1.5×10^8 CFU/mL (CFU: colony forming unit) were prepared in sterile 0.9% NaCl.

Before testing, the minimum inhibitory concentration (MIC) of the hop extract was determined using a turbidity assay by inoculating a bacterial suspension into BHI broth (10 mL) to provide an initial density of 1×10^5 CFU/mL. Concentrations of the hop extract ranged from 0.1 µg/mL to 150 µg/mL. The tubes with each strain were incubated at 37°C for 24 h and growth inhibition was determined by observing the change in turbidity. All experiments were performed in triplicate.

Determination of Growth Inhibition Zones of the H. lupulus Extract

The hop extract was tested initially for its antibacterial activity using the disc diffusion method. Disc samples (6 mm diameter) were prepared from sterile filter paper and impregnated with the hop extract (100 µL) corresponding to 50 µg/disc, then dried for 24 h at room temperature. The discs were placed on the agar surface inoculated with the individual bacterial strain and the plates incubated at 37°C for 24 h depending on the strain used in the test, as indicated previously. After the incubation period, the diameters of the growth inhibition zones were measured using calipers and recorded.

Chlorhexidine gluconate 0.12% (Sigma-Aldrich, St. Louis, MO, USA) was used as the positive control and saline solution as the negative control. Tests were repeated three times to assess reproducibility.

Determination of Growth Inhibition Zones of the Matrices

For the antibacterial activity of the matrices, disc samples (6 mm in diameter) were cut from the electrospun matrices and sterilized by UV radiation for 30 min before placing on the cultured agar plates. The discs of the PCL/nHAp/hop extract were placed on Petri dishes containing the requisite agar, inoculated with the corresponding microorganisms, *S. mutans*, *P. gingivalis*, or *A. actinomycetemcomitans*, and incubated at 35°C for 24 h under anaerobic conditions. The inhibition zones (mm) were measured for each sample. Chlorhexidine gluconate 0.12% was used as the positive control and saline solution as the negative control. All the tests were conducted independently in triplicate experiments.

2.9. Cell Culture and Cell Viability Assay

The viability test was carried out with the Detroit 548 CCL-116 cell line of human skin fibroblasts using the direct contact assay method and following the International Organization for Standardization (1993) protocols [33]. Cells (1×10^4) were seeded in 96-well microplates and incubated for 24 h at 37°C in a 5% CO_2 atmosphere in DMEM (Dulbecco's Modified Eagle Medium) (Gibco, Grand Island, NY, USA) supplemented with 10% fetal bovine serum (Gibco). All the processed matrices were cut into round discs of 5 mm and sterilized under UV light for 30 min, soaked in 70% ethanol for 30 min, then washed twice with PBS.

The sterile discs samples were placed in the 96-wells along with the fibroblasts cells and incubated in DMEM for 48 h at 37°C in a 5% CO_2 atmosphere. After this period, nanofiber samples were removed from the wells and MTT (3-(4,5-dimethylthiazol-2-yl)-2,5-diphenyltetrazolium bromide) reagent (10 µL) was added. After incubation of the cells with MTT for 4 h, the medium with the reagent was withdrawn, and DMSO (100 µL) was added to dissolve the formazan. The optical density (OD) was measured at 570 nm with a Biotek Synergy 2 plate spectrophotometer (Winooski, VT, USA). Cells in contact with the matrices were used as a positive control, and medium with untreated cells was the blank.

The cell viability was calculated according to the following equation:

Cell viability (%) = [(OD of treated cells (with the matrices) – OD of blank)/ (OD of untreated cells – OD of blank)] × 100.

All tests were performed five times in three independent experiments.

2.10. Statistical Analysis

Results are shown as the mean value ± the standard deviation (SD) of the mean. ANOVA analyses of variance followed by a Tukey test were used to compare the differences between groups. Probability values of $p \leq 0.05$ were considered significant. The statistical analysis was performed using IBM SPSS 25.0 (Corporation Business Analytics Software, Chicago, IL, USA) software.

3. Results

3.1. Morphological Characterization

The optimum sample parameters obtained in this work were a polymer concentration of 9%, a nHAp concentration of 3%, and a Humulus lupulus concentration of 3%. The optimized electrospinning parameters were 25 kV voltage, 15 cm distance, and 0.4 mL/h^{-1} flow rate. SEM was used to examine the morphological characteristics of the electrospun nanofibers. According to the statistical analysis, the diameter of the fibers varied based on the presence of the nHAp and the amount of hop extract introduced. All the prepared PCL, PCL+nHAp, and PCL+nHAp+hop extract samples presented homogeneous diameter distribution of the fibers (Figures 1A, 1B, and 1C). According to the SEM micrographs, non-aligned fiber distribution with an interconnected porosity

was observed for all the samples, whereas the presence of nHAp resulted in the occurrence of some bead-like structures (Figures 1B and 1C).
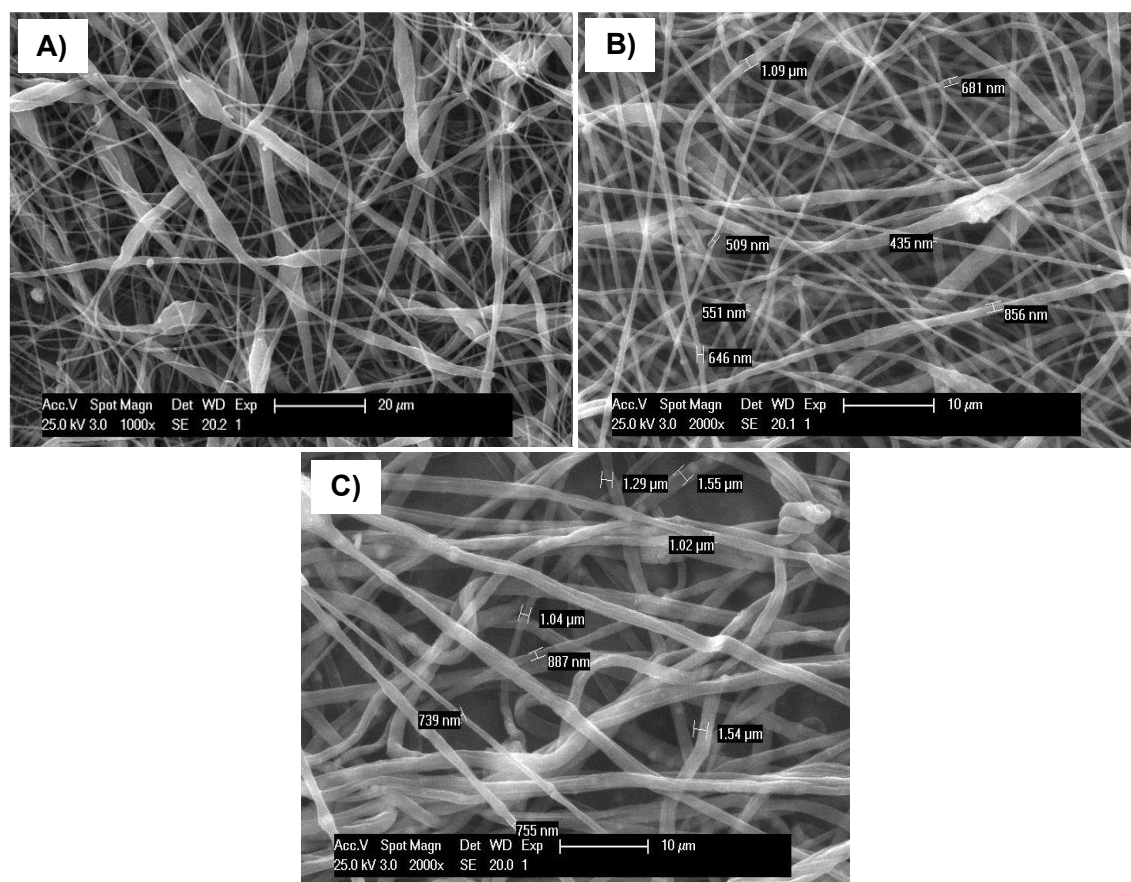

Figure 1. SEM micrographs showing the diameter and distribution of the electrospun fibers of PCL, nHAp, and hop extract: A) PCL; B) PCL+nHAp; and C) PCL+nHAp+hop extract. Median fibers were calculated using more than 100 random fiber positions in three different SEM images.

From a medicinal agent delivery perspective, the electrospinning technique has promoted the development of matrices or scaffolds with plant extracts encapsulated into polymeric nanofibers [34,35]. The processing conditions, such as the polymeric solution viscosity and conductivity, flow rate, voltage, distance between the nozzle and the collector, and the relative humidity each affect formation of the nanofibers. Moreover, even though the viscosity of the polymer solution or the polymer blend was not determined, the increased viscosity due to the hop extract and the nHAp might have contributed to the occurrence of the fiber diameter variation.

Small water droplets present in the atmosphere can also interact with the polymer jet during the process. As a result, these parameters can influence the diameter, morphology, porosity, structure, and mechanical properties of the electrospun fibers [36,37]. In this study, the median size of the PCL fibers without nHAp or the hop extract was 549 nm, while the median diameter of the samples of the PCL and nHAp fibers was 681 nm, and for the fibers with the PCL/nHAp/hop extract the median diameter was 1102 nm. A study by Chong *et al.* [38] showed that the average diameter of PCL fibers without nHAp was 478.5 nm, and with 3% nHAp was increased to 521.1 nm. The statistical analysis performed on the selected SEM samples shows the average diameter of the fibers and the standard deviation. Tukey's test confirmed that there were significant differences among the samples analyzed (Table 1) and demonstrated that incorporation of the hop extract and the nHAp significantly increased the median diameter of the fibers.

Table 1. Median fiber diameter (in nm) of the electrospun matrices.

Sample	Fiber Diameter (nm ± SD)	*p* value
PCL	549 ± 60[a]	0.70
PCL+nHAp	681 ± 112[b]	0.99
PCL+nHAp+hop ext.	1102 ± 162[c]	0.01

Distinct superscript letters indicate statistically significant differences among groups ($p < 0.05$).

Interestingly, the addition of nHAp into the PCL-based solution substantially modified the morphology of the fibers, which became wider compared to the other matrices, probably due to the agglomeration of nHAp particles on the surface and inner structure of the fibers (Figure 1B). In an earlier study by Hassan and Sultana, the PCL membranes showed a fiber diameter of 0.25 ± 0.08 μm, but when 10% of nHAp was added, the fiber diameter increased to an average of 0.65 ± 0.18 μm [39]. This study is in agreement, wherein an increased fiber diameter was observed when nHAp was added.

3.2. Thermogravimetric Analysis (TGA)

The thermogravimetric analyses (TGAs) are shown in Figure 2 and summarized in Table 2. The residual mass of PCL showed a one-step degradation curve and a maximum degradation temperature of 411°C. This result was consistent with previous TGA studies of PCL degradation which presented depolymerization as a single step process since it breaches the thermal stability of PCL [40,41]. The thermal stability shown by nHAp in this study is consistent with previous studies where HAp has degradation temperatures ranging from 1000 to 1500°C [42,43]. Variations in the maximum degradation temperature were attributed to the nHAp concentration. The low nHAp concentration used in this work (3% w/v) increased the PCL thermal degradation, as previously suggested [44,45]. PCL nanofibers manufactured with nHAp presented the highest (22.7%) post-analysis residue compared with the PCL alone and PCL/nHAp/hop samples (0.835% and 19.19%, respectively). In this study, PCL presented a residue of less than 1%, as observed previously [46]. The degradation curves of the analyzed samples are presented in Figure 2.
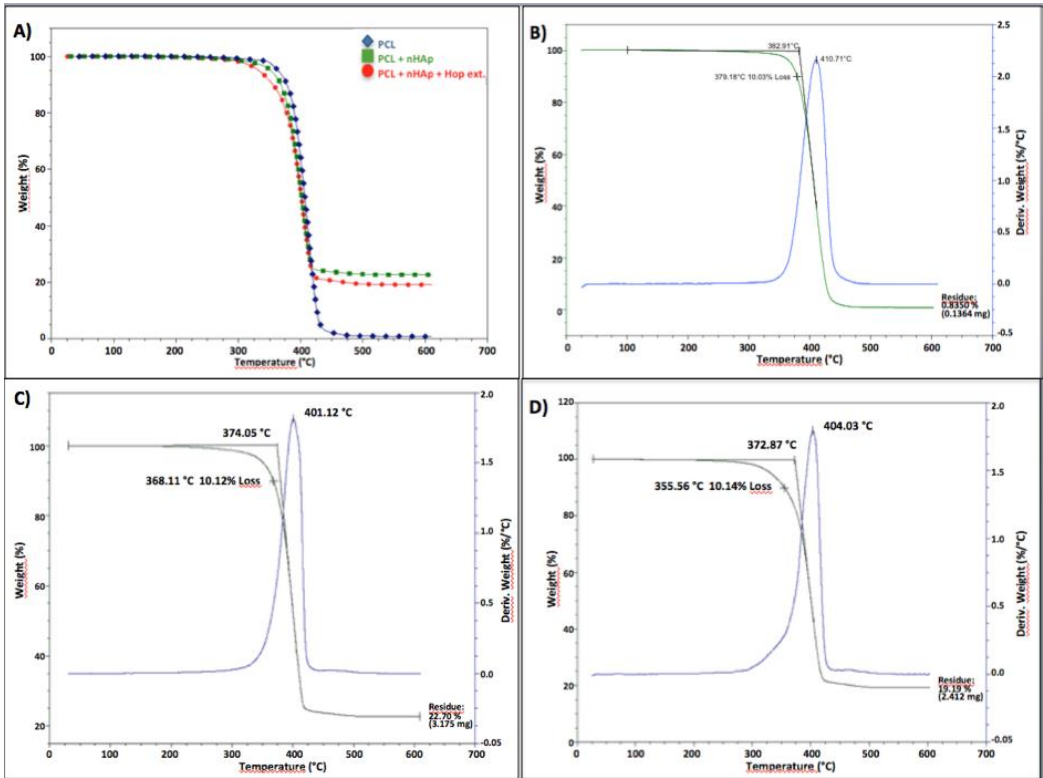
Figure 2. Thermographs of the analyzed matrices. A) The blue line is for the PCL matrices, the green line is for the PCL+nHAp matrices, and the red line is for the PCL+nHAp+hop extract matrices; B) degradation curves of PCL; C) degradation curves of PCL+nHAp; and D) degradation curves of PCL+nHAp + hop extract.

Thermogravimetric analysis of the samples with the hop extract and nHAp show changes in their onset temperature, maximum weight loss temperatures, and in the percentage of waste obtained from the fibers at the end of the analysis (Table 2).

Table 2. Onset temperatures, maximum weight loss temperature, and residue of the processed electrospun matrices. .

Sample	Onset (°C)	Max. weight loss temp (°C)	Residue (%)
PCL	382.91	410.71	0.83
PCL+nHAp	374.05	401.12	22.70
PCL+nHAp+hop ext.	372.87	404.03	19.20

3.3. FTIR Analysis

The Fourier Transform infrared (FTIR) spectra of the different combinations of electrospun matrices are shown in Figure 3A. The parent spectrum shows absorptions bands at 2943 cm^{-1} and 3000 cm^{-1} that correspond to the C-H stretching vibrations of aromatic and aliphatic compounds. The absorption bands at 1240 cm^{-1} and 1723 cm^{-1} correspond to a stretching vibration for the carbonyl (C=O), carbon-hydrogen and (-CH), and C-O-C bonds, respectively, characteristic of PCL [47] (Figure 3B). Furthermore, the major absorptions of a phosphate group (PO4) identified at 1021 cm^{-1} and 564 cm^{-1} were characteristic of nHAp [48]. The infrared spectrum of PCL with nHAp showed similar characteristic peaks (Figures 3B and 3C).

In the FTIR spectrum of the nanofiber samples with the hop extract a carbonyl band (C=O) occurred at 1667 cm^{-1} and at 1600 cm^{-1} for the cyclohexadienone nucleus corresponding to the major compounds of hop: humulone and lupulone [49]. The relatively low intensity of these bands (Figure 3D) is attributed predominantly to the low concentration of hop extract in the matrices, and partially to the molecular interactions between the polymer and the hop extract.
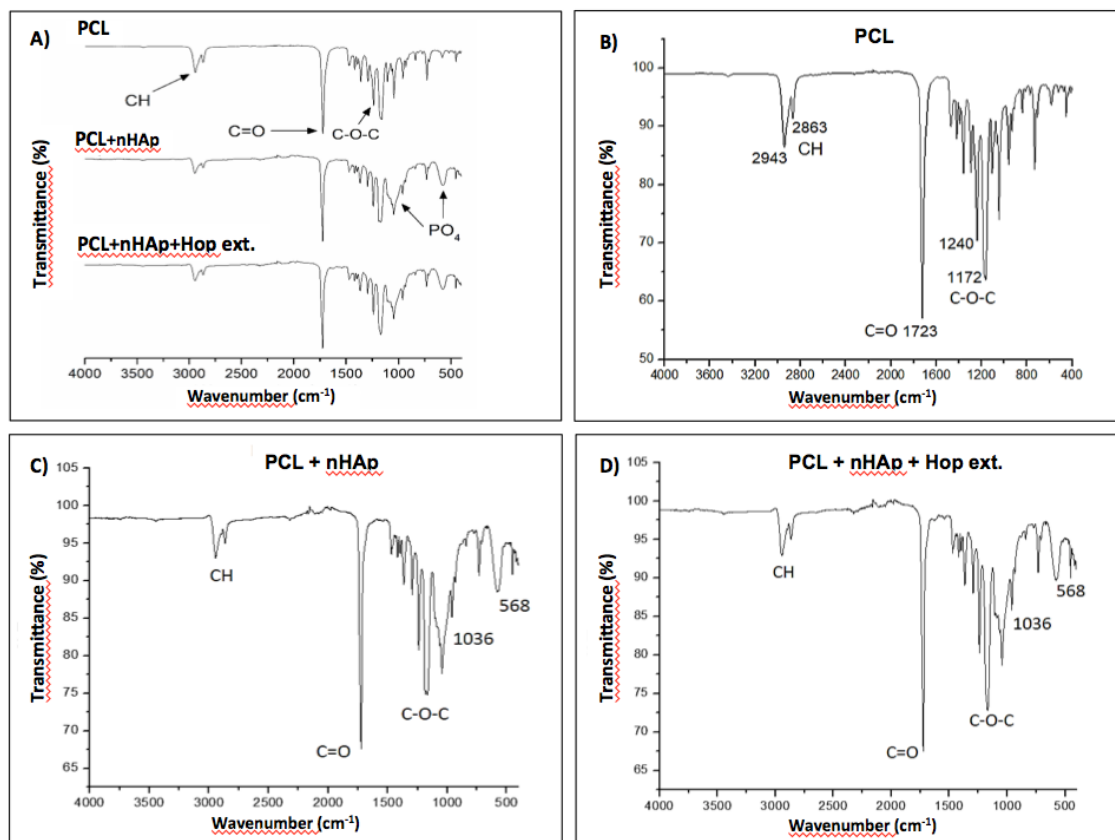
Figure 3. FTIR spectra for the electrospun matrices. 3A): comparison between all the samples; a): PCL; b): PCL+nHAp; and C): PCL+nHAp +hop extract. The arrows show the characteristic absorptions of each material and the functional group assignments. 3B): FTIR spectrum of PCL. 3C): FTIR spectrum of PCL+nHAp. 3D): FTIR spectrum of PCL+nHAp+hop extract.

3.4. In Vitro Degradation Analysis

The hydrolytic degradation test was conducted through immersion of the samples into sterile flasks containing 100 mL of PBS at 37ºC with constant agitation at 120 rpm (to simulate physiological conditions) for 8 weeks. The fibers that only contained PCL showed a 1% mass loss percentage after 8 weeks. Figure 4 shows the aspects of the two samples following the immersion period.

Figure 4. Electrospun matrices. A) PCL only sample, B) PCL+nHAp+hop extract sample after 8 weeks of immersion in PBS at 37°C with constant agitation at 120 rpm and a pH of 7.4.

The *in vitro* degradation rate was consistent with a previous study of PCL characterization where molecular weight (Mw 80,000), crystallinity, pH, and temperature were influential factors [50]. The fibers with PCL, nHAp, and the hop extract showed degradation rates of 1%, 2%, and 4%, respectively after 8 weeks, as shown in Table 3. The incorporation of both nHAp and the hop extract causes water diffusion into the amorphous regions of PCL increasing its hydrolytic degradation. Consequently, more extensive hydrolysis of nanofibers occurred compared to those produced with PCL alone [51], although ANOVA analysis showed that there were no significant differences between the degradation rates of the analyzed samples. The weight difference was observed from the start of the trial until after 8 weeks. Following that period, the samples were washed with distilled water and dried for 24 h at 40°C, and then weighed to constant weight.

Table 3. Differences in weight loss of the electrospun matrices following the 8-week degradation period.

Sample	Initial weight (mg)	Final weight (mg)	Weight loss (%)
PCL	10.13	10.02	1
PCL+nHAp	10.10	9.90	2
PCL+nHAp+hop ext.	10.13	9.70	4

3.5. Mechanical Characterization.

The electrospun matrices were submitted to the tensile strength assay. The results of the Young's modulus and the percentage of elongation to failure are summarized in Table 4. For the sample matrices of PCL alone, PCL+nHAp, and PCL+nHAp+hop extract, the highest values for the mechanical properties were observed for the PCL matrices alone; lower mechanical characteristics were determined for the samples of PCL+nHAp. These variations in the mechanical properties depend on the electrospinning parameters, the diameter and orientation of the fibers, the molecular weight, and the polymer concentration [52]. The addition of nHAp increases the diameter of the PCL nanofibers and decreases the tensile strength. This occurs when the amount of PCL matrices binds the nHAp particles and the stress is transferred between them [53].

In a previous study [54], the tensile strength values for dry PCL scaffolds with oriented nanofibers were 3.8 ± 0.8 MPa and an elongation at break of 170%, while the present results showed a tensile strength and elongation at break of 1.74 ± 0.63 and 3.8%, respectively. The differences between the previous study and this work could be due to the orientation of the fibers (aligned vs. non-aligned), the porosity of the fibers, the diameter of the fibers (250-700 nm – 549 nm), and the interactions between fibers [54].

Table 4. Young's modulus values for the electrospun samples and the percentage of elongation.

Sample	Tensile strength (MPa) (Mean ± SD)	Elongation at break (% ± SD)
PCL	1.74 ± 0.63[a]	3.8 ± 0.66[a]
PCL+nHAp	1.39 ± 0.69[a]	2.2 ± 0.81[a]
PCL+nHAp+hop ext.	1.07 ± 0.35[a]	5.4 ± 1.90[a]

Distinct superscript letters indicate statistically significant differences among groups (p < 0.05).

The results obtained with PCL and nHAp are consistent with a previous study [55] where, by increasing the amount of hydroxyapatite, the percentage tensile deformation of the nanofibers decreases. Other research [56] also demonstrated that, compared with fibers without any plant extract, fibers including a plant extract had a decrease in Young's modulus and variation in the percentage of tensile deformation. This phenomenon also depends on the properties of the natural compounds incorporated into the fibers [57,58], and the increase or decrease in these parameters may be attributed to the different chemical interactions of the metabolites with the polymer [56]. The ANOVA analysis shows that there is no significant difference in the tensile deformation between the analyzed samples.

3.6. Antibacterial Assay

The antimicrobial activity of the commercial Hopsteiner Humulus lupulus extract against oral Gram-positive microorganisms was demonstrated in previous studies [59,60], while it was inactive against oral Gram-negative pathogens [61], with the exception of Phorphyromonas gingivalis [25].

Previous data have shown that H. lupulus possesses antimicrobial activity against Streptococcocus spp. with a minimum inhibitory concentration (MIC) of 0.39 μg/mL [62]. In the present work, the commercial H. lupulus extract was evaluated at 3% against Gram-positive (Streptococcocus mutans), and Gram-negative periodontal pathogens (P. gingivalis and A. actinomycetemcomitans).

Determination of Growth Inhibition Zones

The disc diffusion method is a sensitive and standardized test to quantify the ability of antibiotics to inhibit bacterial growth. It has been suggested that the flavonoids and polyphenols contained in the H. lupulus extracts, such as the α- and β-acids and xanthohumol, are likely responsible for the growth inhibition of Gram-positive [63] and Gram-negative bacteria [64]. In this work, a commercial extract of H. lupulus that contains α-acids, β-acids, and other compounds was used.

The present study provides evidence for the antibacterial effects of the hop extract on the oral pathogenic organisms S. mutans, P. gingivalis, and A. actinomycetemcomitans using filter paper discs impregnated with the hop extract (100 μL). The results showed inhibition zone diameters of 19 mm for S. mutans, 15 mm for P. gingivalis, and 12 mm for A. actinomycetemcomitans. Also, in this study, all the strains showed growth inhibition when they were exposed to 0.12% chlorhexidine gluconate with halo zones of 28 mm, 25 mm, and 23 mm, respectively. The zones of bacterial growth inhibition are summarized in Table 5.

Table 5. Zones of bacterial growth inhibition (mm) produced by the chlorhexidine, hop extract, and the PCL matrices with nHAp and with hop extract.

Sample	Inhibition zone (mm) ±SD		
	Sm	*Pg*	*Aa*
Chlorhexidine 0.12% (+ control)	28 ± 0.4[a]	25 ± 2.1[a]	23 ± 0.4[a]
Hop extract	19 ± 0.5[b]	15 ± 0.8[b]	12 ± 4.4[b]
PCL+nHAp+hop ext.	4 ± 1.2[c]	2 ± 1.7[c]	0 ± 0.5[c]

Distinct superscript letters indicate statistically significant differences among groups ($p < 0.05$).

In the studies of Gregory et al. [63], ten different commercial hop extracts were evaluated against Streptococcus mutans biofilm formation. The best results were for two extracts that showed a significant inhibition of biofilm formation at a 1:256 dilution [63]. Another study described the

protective activity of a hop extract on the viability of periodontal ligament cells when they were infected with P. gingivalis [65]. In addition, a clinical study performed in human volunteers showed that the use of a mouth rinse containing a 0.1% hop polyphenol mixture applied five times a day significantly decreased the accumulation of microbial plaque on the teeth surface [66].
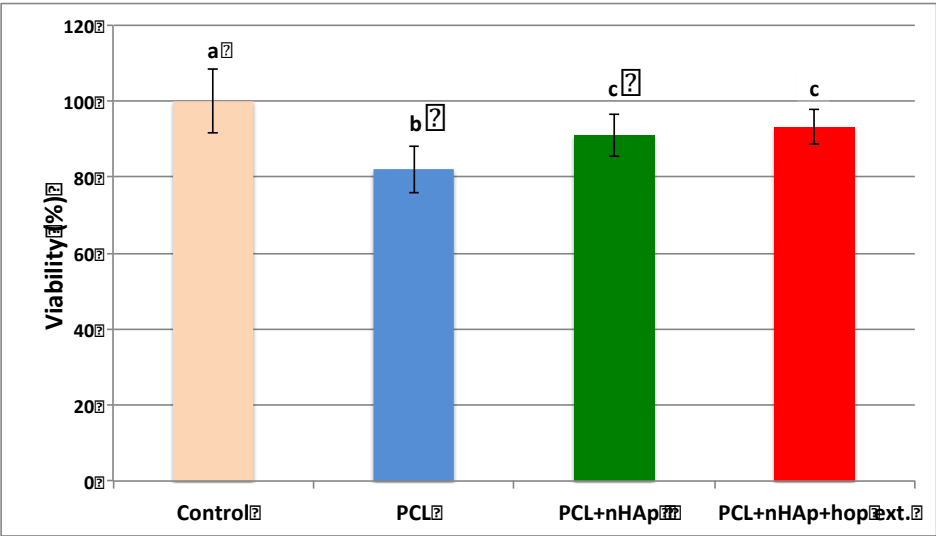
Determination of Growth Inhibition Zones of the Matrices

As indicated in Table 5, the results from the matrices showed zones of growth inhibition of 4 mm for S. mutans and 2 mm for P. gingivalis, and no activity against A. actinomycetemcomitans. This very low antimicrobial activity against the oral pathogens could be attributed to the low amount (3% v/v) of hop extract used to fabricate the polymeric matrices. In another study, higher concentrations of the hop extract were used to obtain an antimicrobial effect [59]. Another possible cause for the weak antimicrobial activity of the matrices against the oral pathogens may be that the hop metabolites can be degraded and oxidized with the UV irradiation during the sterilization process [67] or the release of the extract from the matrix may be limited.

3.7. Cytotoxicity Assay

The most common solvents used to dissolve polycaprolactone are dichloromethane (DCM), trifluoroethanol, and dimethyl formamide (DMF). However, these solvents are toxic to the upper respiratory tract and eyes and require safety precautions when used during the electrospinning process [68]. That was the most important reason to utilize acetone in this work to avoid those risks. The cytotoxicity assessments of the samples were performed using human fibroblasts and applying the MTT assay.

All of the samples tested in this work showed non-cytotoxic activity, with equal viability percentages of the human skin fibroblasts after being in contact with the matrices (Table 6). This confirms previous research where the PCL and nHAp nanofibers were shown to be non-cytotoxic, biocompatible materials [68,69]. Additionally, the fibers containing the H. lupulus extract did not show any cytotoxic effects on human skin fibroblasts after 48 h exposure, indicating that they represent favorable cell biocompatible materials, and confirming the previously reported results [70]. Figure 5 shows the viability of the fibroblasts after being exposed to the PCL+nHAp+hop extract matrices. According to the ISO 10993-5 each of the matrices presented a cell viability higher than 70%, which means that all were cytocompatible [33].

Sample	Viability (%)	± SD
Fibroblasts and DMEM (Control)	100	8.3[a]
PCL	82.15	6.2[b]
PCL+nHAp	91.03	5.5[c]
PCL+nHAp+hop ext.	93.24	4.5[c]

Figure 5. Graph and inset table showing the mean and standard deviation (±SD) of the percentage viability (N=4) of the human skin fibroblasts cultured on the electrospun matrices. Distinct lowercase letters after the standard deviation indicate statistically significant differences between the matrices samples ($p<0.05$).

The limitations of the study include a need to establish the stability of the metabolites of *H. lupulus* through metabolomics, analyzing the release of the metabolites from the matrix in the biological assays. Another limitation in achieving controlled drug delivery under *in vitro* conditions is that PCL presents a low degradation and slow drug release due to its high hydrophobicity. To overcome those limitations, we propose the PCL surface modification and to encapsulate the hop extract into liposomes or nanoparticles to prevent the lost of the compounds release and to improve their bioavailability. Also, the evaluation of the degree of PCL+nHAp crystallinity must be performed to evaluate their mechanical properties and the degradation behavior.

4. Conclusions

This study demonstrated that nHAp and the *H. lupulus* extract can be successfully co-incorporated into PCL electrospun fibers. The mixture of PCL, nHAp, and the H. lupulus extract showed differences in physicochemical properties, indicating that the properties of the matrix can be modulated by adding different concentration of nHAp and/or the hop extract. However, the low concentration of hop extract (3%) incorporated to the PCL matrices only showed weak antimicrobial activity against *S. mutans* and *P. gingivalis* and did not inhibit the growth of *A. actinomycetemcomitans*. Increasing the concentration of the hop extract and evaluating the kinetic release of its constituents from the PCL matrices through HPLC chromatography over a two-month period to determine if the extract release is sustained are proposed for further studies.

The incorporation of the extract and nHAp and the elaboration of the electrospun nanofibers open a window of possibilities for the fabrication of membranes with natural compounds as potential materials for the delivery of medicinal agents and for bone tissue regeneration in various applications once the delivery of an effective dose of the bioactive material can be realized.

Abbreviations

FT-IR   Fourier transform infrared spectroscopy
Hop   Humulus lupulus L.
nHAp   Nano-hydroxyapatite
PBS   Phosphate-buffered saline
PCL   Poly(ε-caprolactone)
SEM   Scanning Electron Microscope
TGA   Thermogravimetric Analysis (TGA)

Conflicts of Interest: The authors declare no conflicts of interest.

References

1. Khademhosseini, A.; Langer, R. Nanobiotechnology - drug delivery and tissue engineering. *Chem. Eng. Prog.* **2006**, *102*, 38–42.
2. Carvalho, M. S.; Cabral, J.; da Silva, C. L.; Vashishth, D. Bone matrix non-collagenous proteins in tissue engineering: creating new bone by mimicking the extracellular matrix. *Polymers.* **2021**, *13*, 1095.
3. Bernard, M.; Jubeli, E.; Pungente, M. D.; Yagoubi, N. Biocompatibility of polymer-based biomaterials and medical devices – regulations, *in vitro* screening and risk-management. *Biomater. Sci.* **2018**, *6*, 2025–2053.
4. Rezaei Kolarijani, N.; Cheraghali, D.; Khastar, H.; Ehterami, A.; Alizade, M.; Vaez, A.; ... & Salehi, M. Nanofibrous polycaprolactone/gelatin scaffold containing gold nanoparticles: Physicochemical and biological characterization for wound healing. *Wound Repair Regen.* **2023**, *31*, 804–815.
5. Lykins, W. R.; Bernards, D. A.; Schlesinger, E. B.; Wisniewski, K.; Desai, T. A. Tuning polycaprolactone degradation for long acting implantables. *Polymer.* **2022**, *262*, 125473–125480.
6. Rahimkhoei, V., Padervand, M., Hedayat, M., Seidi, F., Dawi, E. A., & Akbari, A. Biomedical applications of electrospun polycaprolactone-based carbohydrate polymers: A review. *Int. J. Biol. Macromol.* **2023**, 126642.
7. Halim, N. A. A.; Hussein, M. Z.; Kandar, M. K. Nanomaterials - upconverted hydroxyapatite for bone tissue engineering and a platform for drug delivery. *Int. J. Nanomed.* **2021**, *16*, 6477.
8. Munir, M. U.; Salman, S.; Javed, I.; Bukhari, S. N. A.; Ahmad, N.; Shad, N. A.; Aziz, F. Nano-hydroxyapatite as a delivery system: overview and advancements. *Artif. Cells, Nanomed. Biotechnol.* **202**1, *49*, 717–727.
9. Du, M.; Chen, J.; Liu, K.; Xing, H.; Song, C. Recent advances in biomedical engineering of nano-hydroxyapatite including dentistry, cancer treatment and bone repair. *Compos. B. Eng.* **2021**, *215*, 108790.
10. Haider, M. K.; Kharaghani, D.; Sun, L.; Ullah, S.; Sarwar, M. N.; Ullah, A.; Khatri, M.; Yoshiko, Y.; Gopiraman, M.; Kim, I. S. Synthesized bioactive lignin nanoparticles/polycaprolactone nanofibers: A novel nanobiocomposite for bone tissue engineering. *Biomater. Adv.* **2023**, *144*, 213203.
11. Hussain, Z., Mehmood, S., Liu, X., Liu, Y., Wang, G., Pei, R. Decoding bone-inspired and cell-instructive cues of scaffolds for bone tissue engineering. *Eng. Regen.* **2023**, *5*, 21–44.
12. Zhao, Y.; Fan, T.; Chen, J.; Su, J.; Zhi, X.; Pan, P.; Zou, L.; Zhang, Q. Magnetic bioinspired micro/nanostructured composite scaffold for bone regeneration. *Colloids Surf. B Biointerfaces.* **2019**, *174*, 70–79.
13. Hoveidaei, A. H.; Sadat-Shojai, M.; Mosalamiaghili, S.; Salarikia, S. R.; Roghani-Shahraki, H.; Ghaderpanah, R.; Ersi, M. H.; Conway, J. D. Nano-hydroxyapatite structures for bone regenerative medicine: Cell-material interaction. Bone. 2023, 116956.
14. Awad, H. A.; O'Keefe, R. J.; Mao, J. J. Bone tissue engineering. In: Principles of Tissue Engineering, Elsevier: Oxford, UK, 2020; pp. 1511–1519.
15. Slots, J. Periodontitis: facts, fallacies and the future. *Periodontology 2000.* **2017**, *75*, 7–23.
16. Hamada, S.; Slade, H. D. Biology, immunology, and cariogenicity of *Streptococcus mutans. Microbiol. Rev.* **1980**, *44*, 331–384.
17. He, M.; Wang, Q.; Xie, L.; Wu, H.; Zhao, W.; Tian, W. Hierarchically multi-functionalized graded membrane with enhanced bone regeneration and self-defensive antibacterial characteristics for guided bone regeneration. *Chem. Eng. J.* **2020**, *398*, 125542.
18. Li, J.; Lai, Y.; Li, M.; Chen, X.; Zhou, M.; Wang, W.; Li, J.; Cui, W.; Zhang, G.; Liu, L.; Lin, Y. Repair of infected bone defect with clindamycin-tetrahedral DNA nanostructure complex-loaded 3D bioprinted hybrid scaffold. *Chem. Eng. J.* **2022**, 134855.
19. Song, M.; Liu, Y.; Li, T.; Liu, X.; Hao, Z.; Ding, S., Panichayupakaranan, P.; Zhu, K.; Shen, J. Plant natural flavonoids against multidrug resistant pathogens. *Adv. Sci.* **2021**, *8*, 2100749.
20. Abiko, Y.; Paudel, D.; Uehara, O. Hops components and oral health. *J. Funct. Foods.* **2022**, *92*, 105035.
21. González-Salitre, L.; González-Olivares, L. G.; Basilio-Cortes, U. A. *Humulus lupulus* L. a potential precursor to human health: High hops craft beer. *Food Chem.* **2023**, *405*, 134959.

22. Betancur, M.; López, J.; Salazar, F. Antimicrobial activity of compounds from hop (*Humulus lupulus* L.) following supercritical fluid extraction: An overview. *Chil. J. Agric. Res.* **2023**, *83*, 499-509.

23. Khaliullina, A.; Kolesnikova, A.; Khairullina, L.; Morgatskaya, O.; Shakirova, D.; Patov, S.; Nekrasova, P.; Bogachev, M.; Kurkin, V.; Trizna, E.; Kayumov, A. The antimicrobial potential of the hop (*Humulus lupulus* L.) extract against *Staphylococcus aureus* and oral Streptococci. *Pharmaceuticals.* **2024**, *17*, 162.

24. Bolton, J. L.; Dunlap, T. L.; Hajirahimkhan, A.; Mbachu, O.; Chen, S.-N.; Chadwick, L.; Nikolic, D.; van Breemen, R. B.; Pauli, G. F.; Dietz, B. M. The multiple biological targets of hops and bioactive compounds. *Chem. Res. Toxicol.* **2019**, *32*, 222–233.

25. Hiraki, D.; Uehara, O.; Harada, F.; Takai, R.; Takahasi, S.; Taraya, S.; Abiko, Y. Effect of xanthohumol on *Porphyromonas gingivalis. Jpn. J. Conserv. Dent.* **2019**, *62*, 271–278.

26. Harish, V.; Haque, E.; Śmiech, M.; Taniguchi, H.; Jamieson, S.; Tewari, D.; Bishayee, A. Xanthohumol for human malignancies: chemistry, pharmacokinetics and molecular targets. *Int. J. Mol. Sci.* **2021**, *22*, 4478.

27. Jeong, H. M.; Han, E. H.; Jin, Y. H.; Choi, Y. H.; Lee, K. Y.; Jeong, H. G. Xanthohumol from the hop plant stimulates osteoblast differentiation by RUNX2 activation. *Biochem. Biophys. Res. Commun.* **2011**, *409*, 82–89.

28. Abdul Hameed, M. M.; Mohamed Khan, S. A. P.; Thamer, B. M.; Rajkumar, N.; El-Hamshary, H.; El-Newehy, M. Electrospun nanofibers for drug delivery applications: Methods and mechanism. *Polym. Adv. Technol.* **2023**, *34*, 6–23.

29. Liu, H.; Bai, Y.; Huang, C.; Wang, Y.; Ji, Y.; Du, Y.; Bligh, S. W. A. Recent progress of electrospun herbal medicine nanofibers. *Biomolecules.* **2023**, *13*, 184.

30. Liu, J.; Zou, Q.; Wang, C.; Lin, M.; Li, Y.; Zhang, R.; Li, Y. Electrospinning and 3D printed hybrid bi-layer scaffold for guided bone regeneration. *Mater. Des.* **2021**, *210*, 110047.

31. ISO. Biological evaluation of medical devices - Part 13: Identification and quantification of degradation products from polymeric medical devices; ISO 10993-13; ISO: Geneva, Switzerland 2010.

32. Bauer, A. W. Antibiotic susceptibility testing by a standardized single disc method. *Am. J. Clin. Pathol.* **1966**, *45*, 149–158.

33. ISO. Biological Evaluation of Medical Devices. Part 5: Tests for Cytotoxicity: I*n Vitro* Methods; ISO 10993-5; ISO: Geneva, Switzerland 1993.

34. Zhu, P.; Yin, H.; Wei, J.; Wu, J.; Ping, D.; Zhang, X. A bilayer biocompatible polycaprolactone/zinc oxide/*Capparis spinosa* L. ethyl acetate extract/polylactic acid nanofibrous composite scaffold for novel wound dressing applications. *Int. J. Biol. Macromol.* **2023**, 125093.

35. Irani, M.; Abadi, P. G.; Ahmadian-Attari, M. M.; Rezaee, A.; Kordbacheh, H.; Goleij, P. *In vitro* and *in vivo* studies of Dragon's blood plant (*D. cinnabari*)-loaded electrospun chitosan/PCL nanofibers: Cytotoxicity, antibacterial, and wound healing activities. *Int. J. Biol. Macromol.* **2024**, *257*, 128634.

36. Szewczyk, P. K.; Stachewicz, U. The impact of relative humidity on electrospun polymer fibers: from structural changes to fiber morphology. *Adv. Colloid Interfac. Sci.* **2020**, *286*, 102315.

37. Ahmadi Bonakdar; M., Rodrigue, D. Electrospinning: processes, structures, and materials. *Macromolecules.* **2024**, *4, 58*–103.

38. Chong, L. H.; Hassan, M. I.; Sultana, N. Electrospun polycaprolactone (PCL) and PCL/nano-hydroxyapatite (PCL/nHA)-based nanofibers for bone tissue engineering application. In: *IEEE 10th Asian Control Conference (ASCC), Malaysia,* **2015**, 1–4.

39. Hassan, M. I.; Sultana, N. Characterization, drug loading and antibacterial activity of nanohydroxyapatite/polycaprolactone (nHA/PCL) electrospun membrane. *3 Biotech.* **2017**, *7*, 1–9.

40. Fortună, M. E.; Ungureanu, E.; Rotaru, R.; Bargan, A.; Ungureanu, O. C.; Brezuleanu, C. O.; Harabagiu, V. Synthesis and properties of modified biodegradable polymers based on caprolactone. *Polymers.* **2023**, *15*, 4731.

41. Emadi, H.; Karevan, M.; Masoudi Rad, M.; Sadeghzade, S.; Pahlevanzadeh, F.; Khodaei, M.; Khayatzadeh, S.; Lotfian, S. Bioactive and biodegradable polycaprolactone-based nanocomposite for bone repair applications. *Polymers.* **2023**, *15*, 3617.

42. Yu, P.; Huang, S.; Yang; Z., Liu; T.; Qilin, Z.; Feng, J.; Zeng, B. Biomechanical properties of a customizable TPU/PCL blended esophageal stent fabricated by 3D printing. *Mater. Today Commun.* **2023**, *34*, 105196.

43. Su, T. T.; Jiang, H.; Gong, H. Thermal stabilities and the thermal degradation kinetics of poly(ε-caprolactone). *Polym-Plast. Technol. Eng.* **2008**, *47*, 398–403.

44. Motloung, M. P.; Mofokeng, T. G.; Ray, S. S. Viscoelastic, thermal, and mechanical properties of melt-processed poly(ε-caprolactone) (PCL)/hydroxyapatite (HAP) composites. *Materials.* **2021**, *15*, 104.

45. Dias, D.; Vale, A. C.; Cunha, E. P.; C Paiva, M.; Reis, R. L., Vaquette, C.; Alves, N. M. 3D-printed cryomilled poly(ε-caprolactone)/graphene composite scaffolds for bone tissue regeneration. *J. Biomed. Mater. Res. -B: Appl. Biomater.* **2021**, *109*, 961–972.

46. Loyo, C.; Cordoba, A.; Palza, H.; Canales, D.; Melo, F.; Vivanco, J. F.; Vallejos R.; Millán, C.; Corrales, T.; Zapata, P. A. Effect of Gelatin Coating and GO incorporation on the properties and degradability of electrospun PCL scaffolds for bone tissue regeneration. *Polymers*. **2023**, *16*, 129.

47. Alexeev, D.; Tschopp, M.; Helgason, B.; Ferguson, S. J. Electrospun biodegradable poly(ε-caprolactone) membranes for annulus fibrosus repair: Long-term material stability and mechanical competence. *JOR Spine*. **202**1, *4*, e1130.

48. Swetha, S.; Balagangadharan, K.; Lavanya, K.; Selvamurugan, N. Three-dimensional-poly(lactic acid) scaffolds coated with gelatin/magnesium-doped nano-hydroxyapatite for bone tissue engineering. *Biotechnol. J.* **2021**, *16*, 2100282.

49. Masek, A.; Chrzescijanska, E.; Kosmalska, A.; Zaborski, M. Characteristics of compounds in hops using cyclic voltammetry, UV–VIS, FTIR and GC–MS analysis. *Food Chem.* **2014**, *156*, 353−361.

50. Pawar, R.; Pathan, A.; Nagaraj, S.; Kapare, H.; Giram, P.; Wavhale, R. Polycaprolactone and its derivatives for drug delivery. *Polym. Adv. Technol*. **2023**, *34*, 3296−3316.

51. Yaseri, R.; Fadaie, M.; Mirzaei, E.; Samadian, H.; Ebrahiminezhad, A. Surface modification of polycaprolactone nanofibers through hydrolysis and aminolysis: a comparative study on structural characteristics, mechanical properties, and cellular performance. *Sci. Rep*. **2023**, *13*, 9434.

52. Alharbi, N.; Daraei, A.; Lee, H.; Guthold, M. The effect of molecular weight and fiber diameter on the mechanical properties of single, electrospun PCL nanofibers. *Mater. Today Commun*. **2023**, *35*, 105773.

53. Fu, S. Y.; Feng, X. Q.; Lauke, B.; Mai, Y. W. Effects of particle size, particle/matrix interface adhesion and particle loading on mechanical properties of particulate–polymer composites. *Composites Part B: Eng*. **2008**, *39*, 933−961.

54. Croisier, F.; Duwez, A. S.; Jérôme, C.; Léonard, A. F.; Van Der Werf, K. O.; Dijkstra, P. J.; Bennink, M. L. Mechanical testing of electrospun PCL fibers. *Acta Biomater*. **2012**, *8*, 218−224.

55. Alharbi, N.; Daraei, A.; Lee, H.; Guthold, M. The effect of molecular weight and fiber diameter on the mechanical properties of single, electrospun PCL nanofibers. *Mater. Today Commun.* **2023**, *35*, 105773.

56. Modiri-Delshad, T.; Ramazani, A.; Khoobi, M.; Akbari Javar, H.; Akbari, T.; Amin, M. Fabrication of chitosan/polycaprolactone/*Myrtus communis* L. extract nanofibrous mats with enhanced antibacterial activities. *Polym. Polym. Compos*. **2023**, *31*, 09673911231151506.

57. Moraczewski, K.; Stepczyńska, M.; Malinowski, R.; Karasiewicz, T.; Jagodziński, B.; Rytlewski, P. Modification of polycaprolactone with plant extracts to improve the aging resistance. *Materials*. **2023**, *16*, 5154.

58. Pedram Rad, Z.; Mokhtari J.; Abbasi M. Preparation and characterization of *Calendula officinalis*-loaded PCL/gum Arabic nanocomposite scaffolds for wound healing applications. *Iran. Polym. J*. **2019**, *28*, 51–63.

59. Bhattacharya, S; Virani, S; Zavro, M; Haas, G. J. Inhibition of *Streptococcus mutans* and other oral Streptococci by hop (*Humulus lupulus* L.) constituents. *Econ. Bot.* **2003**, *57*, 118−125.

60. Haas, G.J.; Barsoumian, R. Antimicrobial activity of hop resins. *J. Food Prot.* **1994**, *57*, 59–61.

61. Teuber, M. Low antibiotic potency of isohumulone. *Appl. Microbiol.* **1970**, *19*, 871.

62. Klimek, K.; Tyśkiewicz, K.; Miazga-Karska, M.; Dębczak, A.; Rój, E.; Ginalska, G. Bioactive compounds obtained from Polish "Marynka" hop variety using efficient two-step supercritical fluid extraction and comparison of their antibacterial, cytotoxic, and anti-proliferative activities *in vitro*. *Molecules*. **2021**, *26*, 2366.

63. Gregory, E. R.; Bakhaider, R. F.; Gomez, G. F.; Huang, R.; Moser, E. A.; Gregory, R. L. Evaluating hop extract concentrations found in commercial beer to inhibit *Streptococcus mutans* biofilm formation. *J. Appl. Microbiol.* **2022**, *133*, 1333−1340.

64. Stompor, M.; Żarowska, B. Antimicrobial activity of xanthohumol and its selected structural analogues. *Molecules*. **2016**, *21*, 608.

65. Inaba, H; Tagashira, M; Kanda, T; Ohno, T; Kawai, S; Amano, A. Apple- and hop-polyphenols protect periodontal ligament cells stimulated with enamel matrix derivative from *Porphyromonas gingivalis*. *J. Periodontol.* **2005**, *76*, 2223−2229.

66. Shinada, K; Tagashira, M; Watanabe, H. Hop bract polyphenols reduced three-day dental plaque regrowth. *J. Dent. Res.* **2007**, *86*, 848−851.

67. DeSimone, E.; Aigner, T. B.; Humenik, M.; Lang, G.; Scheibel, T. Aqueous electrospinning of recombinant spider silk proteins. *Mater. Sci. Eng. C*. **2020**, *106*, 110145.

68. Dalton, P.D.; Klinkhammer, K.; Salber, J.; Klee, D.; Möller M. Direct *in vitro* electrospinning with polymer melts. *Biomacromolecules*. **2006**, *13*, 686−90.

69. Lim, M. M.; Sun, T.; Sultana, N. *In vitro* biological evaluation of electrospun polycaprolactone/gelatine nanofibrous scaffold for tissue engineering. *J. Nanomater*. **2015**, *16*, 416.

70. Safaeijavan, R.; Soleimani, M.; Divsalar, A.; Eidi, A.; Ardeshirylajimi, A. Biological behavior study of gelatin coated PCL nanofiberous electrospun scaffolds using fibroblasts. *J. Paramed. Sci.* **2014**, *5*.

71. Philips, N; Samuel, P; Lozano, T; Gvaladze, A.; Guzman, B.; Siomyk, H.; Haas, G. Effects of *Humulus lupulus* extract or its components on viability, lipid peroxidation, and expression of vascular endothelial growth factor in melanoma cells and fibroblasts. *J. Clin. Res.* **2017**, *1*, 15–19.